J Chin Med Assoc

ORIGINAL ARTICLE

TRIM72 mediates lung epithelial cell death upon hyperoxia exposure

Liang-Ti Huang[a,b], Hsiu-Chu Chou[c], Chung-Ming Chen[b,d,*]

[a]Department of Pediatrics, Wan Fang Hospital, Taipei Medical University, Taipei, Taiwan, ROC; [b]Department of Pediatrics, School of Medicine, College of Medicine, Taipei Medical University, Taipei, Taiwan, ROC; [c]Department of Anatomy and Cell Biology, School of Medicine, College of Medicine, Taipei Medical University, Taipei, Taiwan, ROC; [d]Department of Pediatrics, Taipei Medical University Hospital, Taipei, Taiwan, ROC

Abstract

Background: Premature infants often require oxygen (O_2) therapy for respiratory distress syndrome; however, excessive use of O_2 can cause clinical conditions such as bronchopulmonary dysplasia. Although many treatment methods are currently available, they are not effective in preventing bronchopulmonary dysplasia. Herein, we explored the role of tripartite motif protein 72 (TRIM72), a factor involved in repairing alveolar epithelial wounds, in regulating alveolar cells upon hyperoxia exposure.

Methods: In this *in vivo* study, we used Sprague–Dawley rat pups that were reared in room air or 85% O_2 for 2 weeks after birth. The lungs were excised for histological analyses, and TRIM72 expression was assessed on postnatal days 7 and 14. For *in vitro* experiments, RLE-6TN cells (i.e., rat alveolar type II epithelial cells) and A549 cells (i.e., human lung carcinoma epithelial cells) were exposed to 85% O_2 for 5 days. The cells were then analyzed for cell viability, and TRIM72 expression was determined.

Results: Exposure to hyperoxia reduced body and lung weight, increased mean linear intercept values, and upregulated TRIM72 expression. *In vitro* study results revealed increased or decreased lung cell viability upon hyperoxia exposure depending on the suppression or overexpression of TRIM72, respectively.

Conclusion: Hyperoxia upregulates TRIM72 expression in neonatal rat lung tissue; moreover, it initiates TRIM72-dependent alveolar epithelial cell death, leading to hyperoxia-induced lung injury.

Keywords: Alveolar epithelial cells; Cell survival; Hyperoxia; Lung injury; Newborn respiratory distress syndrome

1. INTRODUCTION

Respiratory distress syndrome is a major cause of morbidity and mortality in preterm neonates.[1] During respiratory distress syndrome and respiratory failure, oxygen (O_2) supplementation is mostly indicated to sustain tissue oxygenation. However, preterm infants who have received prolonged O_2 therapy may experience several complications, such as retinopathy of prematurity and bronchopulmonary dysplasia (BPD). BPD continues to be a major cause of morbidity and mortality during the first year of life, and many infants frequently experience more respiratory morbidities, including a decreased response to acute hypoxia and development of obstructive airway diseases throughout childhood.[2–4] At present, no effective clinical therapies are available to prevent the long-term pulmonary sequelae of BPD. Advancements in surfactant and steroid therapy and ventilation strategies have changed the pathological landscape from "classic BPD" to "new BPD." "New BPD," a chronic lung disorder in extremely premature infants, is characterized by lung injury that results in abnormal lung architecture marked more by alveolar and capillary hypoplasia and less by fibroproliferative airway damage and parenchymal fibrosis.[5] Lung injury in animal models has been shown to be similar to pulmonary injury in infants receiving supplemental O_2 therapy.[6–8] The lungs of neonatal rats exposed to a hyperoxic environment were found to have decreased alveolar septation and increased terminal air space size, similar to that observed in classic BPD in humans.[9,10] Hyperoxic injury is believed to disrupt critical signaling pathways that direct lung development, including branching and septation.[5,11,12] Although aberrant regulation of lung development is one of the causative factors of hyperoxia-induced lung injury, the underlying molecular mechanisms remain to be elucidated.

Tripartite motif protein 72 (TRIM72, also known as mitsugumin 53) is abundantly expressed in striated muscle tissues and has been shown to function as a mediator for degradation of the insulin receptor and insulin receptor substrate 1, which is a leading factor in metabolic syndrome.[13] A study reported that S-nitrosylation of TRIM72 at C144 prevented the oxidation-induced degradation of TRIM72 following oxidative insult, consequently enhancing cardiomyocyte survival;[14] another study revealed that TRIM72$^{-/-}$ mice showed increased susceptibility to ischemia–reperfusion and overventilation-induced injury to the lung, concluding that targeting TRIM72-mediated membrane repair in lung epithelial cells could be an effective, integrative component of acute lung injury therapies.[15] Some previous

*Address correspondence. Dr. Chung-Ming Chen, Department of Pediatrics, School of Medicine, College of Medicine, Taipei Medical University, 250, Wu-Hsing Street, Taipei 110, Taiwan, ROC. E-mail address: cmchen@tmu.edu.tw (C.-M. Chen).

Conflicts of interest: The authors declare that they have no conflicts of interest related to the subject matter or materials discussed in this article.

Journal of Chinese Medical Association. (2021) 84: 79-86.

Received April 15, 2020; accepted June 22, 2020.

doi: 10.1097/JCMA.0000000000000413.

studies have also reported the detrimental effects of TRIM72 in cardiac fibrosis and that it causes excessive deposition of extracellular matrix through signaling pathway regulation in myocardial infarction and aortic constriction.[16,17] Thus, under stress conditions, the effects of TRIM72 on experimental targets seem to be both advantageous and disadvantageous. Considering that the role of TRIM72 in lung cells under hyperoxic environments remains unclear, in this study, we investigated the molecular mechanisms responsible for O_2 toxicity, the role of TRIM72 in neonatal murine lung development, and the response of lung tissue cell lines to hyperoxia.

2. METHODS

2.1. Ethical approval

All experiments involving animals were performed in accordance with the animal use protocol enacted by the Institutional Animal Care and Use Committees of School of Medicine, Taipei Medical University.

2.2. Antibodies

The rabbit polyclonal antibody against TRIM72 (GTX 118625) was purchased from GeneTex International Corporation (Irvine, CA, USA). β-Actin mouse mAb (sc-47778) was purchased from Santa Cruz Biotechnology (Santa Cruz, CA, USA). Horseradish peroxidase–conjugated antirabbit and antigoat antibodies were obtained from Invitrogen (Carlsbad, CA, USA), and antimouse antibody was obtained from Thermo Fisher Scientific Inc. (Rockford, IL, USA). Biotinylated antirabbit IgG antibody was purchased from Vector Laboratories (Burlingame, CA, USA).

2.3. Animal models

This study was performed in accordance with the guidelines provided by the Animal Care Use Committee of Taipei Medical University (LAC-2016-0515). Time-dated pregnant Sprague–Dawley rats were housed in individual cages under a 12:12-h light–dark cycle and *ad libitum* access to laboratory food and water. Delivery was performed naturally at term (22 d). Within 12 hours of birth, litters were pooled and randomly redistributed to newly delivered mothers; thereafter, the pups were randomly assigned to room air (normoxia) and O_2 treatment subgroups. The pups in the O_2 treatment subgroup were reared in an atmosphere containing 85% O_2 during postnatal days 1 to 14, and those in the other subgroup were reared under normoxia for 14 postnatal days. Mothers nursing the pups were rotated every 24 hours between the two subgroups to safeguard them from O_2 toxicity. Immediately after death, the lungs were collected for histological analysis, immunohistochemistry, and Western blotting.

2.4. Histological analysis

For standardization, sections from the right middle lobe of the right lung were obtained. Subsequently, the lung tissues were immersed in 4% paraformaldehyde in 0.1 M phosphate buffered saline (pH 7.4), followed by incubation at 4°C for 24 hours. Thereafter, the tissues were dehydrated in alcohol, cleared in xylene, and embedded in paraffin. Five-micrometer sections were stained with hematoxylin and eosin, examined under light microscopy, and assessed for lung morphometry. The mean linear intercept (MLI), an indicator of the mean alveolar diameter, was assessed in 10 nonoverlapping fields.[18]

2.5. Immunohistochemistry

Immunostaining was performed on 5-μm paraffin sections with immunoperoxidase visualization. After blocking endogenous peroxidase activity and nonspecific binding of pertinent antibody, the sections were preincubated for 1 hour at room temperature in 0.1 M phosphate buffered saline containing 10% normal goat serum and 0.3% H_2O_2; subsequently, they were incubated with the primary antibodies of rabbit polyclonal antivon Willebrand factor (vWF) antibody (1:100; ab6994, Abcam, Cambridge, MA, USA) and goat polyclonal anti-TRIM72 (PA5-19398) (1:200 dilutions; Thermo Fisher Scientific, Waltham, MA, USA) for 20 hours at 4°C. The sections were then treated with the secondary antibody of biotinylated rat antigoat IgG (1:200; Jackson ImmunoResearch, West Grove, PA, USA) for 1 hour at 37°C. Subsequently, they were treated with reagents from the avidin–biotin complex kit (Vector Laboratories, Inc., Burlingame, CA, USA), and products were visualized using a diaminobenzidine substrate kit (Vector Laboratories, Inc.), according to manufacturer's instructions. After diaminobenzidine visualization, the sections were lightly counterstained using hematoxylin. All immunostained sections were viewed and photographed using a Nikon Eclipse E600 microscope (Tokyo, Japan).

2.6. Western blotting

Lung tissues and A549 and RLE-6TN cell pellets were lysed in an SDS sample buffer, and the obtained lysates were denatured at 95°C for 10 minutes. Proteins were separated on SDS/polyacrylamide gels and transferred onto polyvinylidene fluoride membranes. The membranes were then blocked with 5% skim milk in Tris-buffered saline containing 0.1% Tween-20 for 30 minutes and incubated overnight with the following primary antibody diluted at 1:1000 to 1:5000 in a blocking solution: rabbit polyclonal antibody against TRIM72 (1:1000; GeneTex International Corporation). β-Actin mouse mAb (1:10000; Santa Cruz Biotechnology) was used as an internal control. The secondary antibodies used were goat antirabbit–Horseradish peroxidase antibody (Jackson, West Grove, PA, USA) against TRIM72 and goat antimouse (#31320) (1:10000; Pierce Biotechnology Inc., Rockford) antibody against β-actin. The densitometry unit for protein expression in the control group was assigned as one after normalization with β-actin.

2.7. Cell culture

Because knockout animal patterns are difficult to achieve and given the unstable tissue condition, we decided to conduct an *in vitro* study. RLE-6TN, a rat alveolar type II epithelial cell line, and A549, a human lung carcinoma epithelial cell line (ATCC, Manassas, VA, USA), were maintained in an F-12 medium in 75-cm^2 tissue culture flasks at 37.8°C in 5% CO_2 and 95% air. Herein, we used two types of lung epithelial cells to compare animal and human alveolar performance. The medium was supplemented with 10% (v/v) fetal bovine serum, 100 U/mL penicillin, and 100 mg/mL streptomycin. Both types of lung cell monolayers were lifted from flasks by adding 2 mL of 0.05% trypsin and then subcultured in 75-cm^2 tissue culture flasks or seeded in 24-well tissue culture plates (BD Labware, Franklin Lakes, NJ, USA) or 4-well chamber slides (Costar Life Sciences, Wilkes Barre, PA, USA) at a density of (12.5-20.0) 3×10^3 cells/well for various experiments. The cells were allowed to attach overnight, transduced with replication-deficient premade TRIM72–green fluorescent protein (GFP) adenovirus (Applied Biological Materials Inc., Richmond, BC, USA) or transfected with lipofectamine RNAiMAX (Thermo Fisher Scientific, Waltham, MA, USA) that contained TRIM72 siRNA (Santa Cruz Biotechnology, Dallas, TX, USA) with the primer TACGTCCAAGGTCGGGCAGGAAGA, and cultured under normoxic (5% CO_2 and 95% air) or O_2-enriched (85% O_2 and 5% CO_2, Xvivo system; BioSpherix, New

Table 1

Body weights, lung weights, and lung-to-body weight ratios of rat pups on postnatal day 7

Treatment	*n*	Body Weight (g)	Lung Weight (g)	Lung-to-Body Weight Ratio (%)
Normoxia	11	15.36 ± 2.86	0.28 ± 0.04	1.85 ± 0.13
O_2	13	9.44 ± 1.71***	0.15 ± 0.02***	1.62 ± 0.16**

Values are presented as mean ± SD.
***$p < 0.001$ vs the normoxia group; **$p < 0.01$ vs the normoxia group.

Table 2

Body weights, lung weights, and lung-to-body weight ratios of rat pups on postnatal day 14

Treatment	*n*	Body Weight (g)	Lung Weight (g)	Lung-to-Body Weight Ratio (%)
Normoxia	11	24.32 ± 1.06	0.38 ± 0.02	1.54 ± 0.10
O_2	13	15.52 ± 1.11***	0.26 ± 0.03***	1.66 ± 0.13*

Values are presented as mean ± SD.
***$p < 0.001$ vs the normoxia group; *$p < 0.05$ vs the normoxia group.

York, NY, USA) conditions in a 30-L direct heat CO_2/Tri-Gas incubator (SA series, ASTEC CO., Fukuoka, Japan) for 48 to 120 hours; the medium was changed every 2 days. All cell culture media, supplements, and chemicals were purchased from Sigma-Aldrich (St. Louis, MI, USA).

2.8. In vitro cell viability assay

After 48, 72, 96, and 120 hours of culture under normoxic or O_2-enriched conditions, cell viability was evaluated by measuring the mitochondrial-dependent reduction of colorless 3-(4,5-dimethylthiazol-2-yl)-2,5-diphenyltetrazolium bromide (MTT; Invitrogen, Eugene, OR, USA) to blue-colored formazan that was dissolved in dimethyl sulfoxide, and the absorbance of each sample was spectrophotometrically measured at 550 nm using a SpectraMax 190 Microplate Reader (Molecular Devices, Downingtown, PA, USA).

2.9. ELISA

A549 and RLE-6TN cell pellets were sonicated and centrifuged. The supernatants were collected, and absorbance was read using a commercial ELISA kit for TRIM72 (Cusabio Biotech Co., Ltd, Houston, TX, USA; CSB-EL024511HU and CSB-EL024511RA). TRIM72 concentration is presented as optical density values.

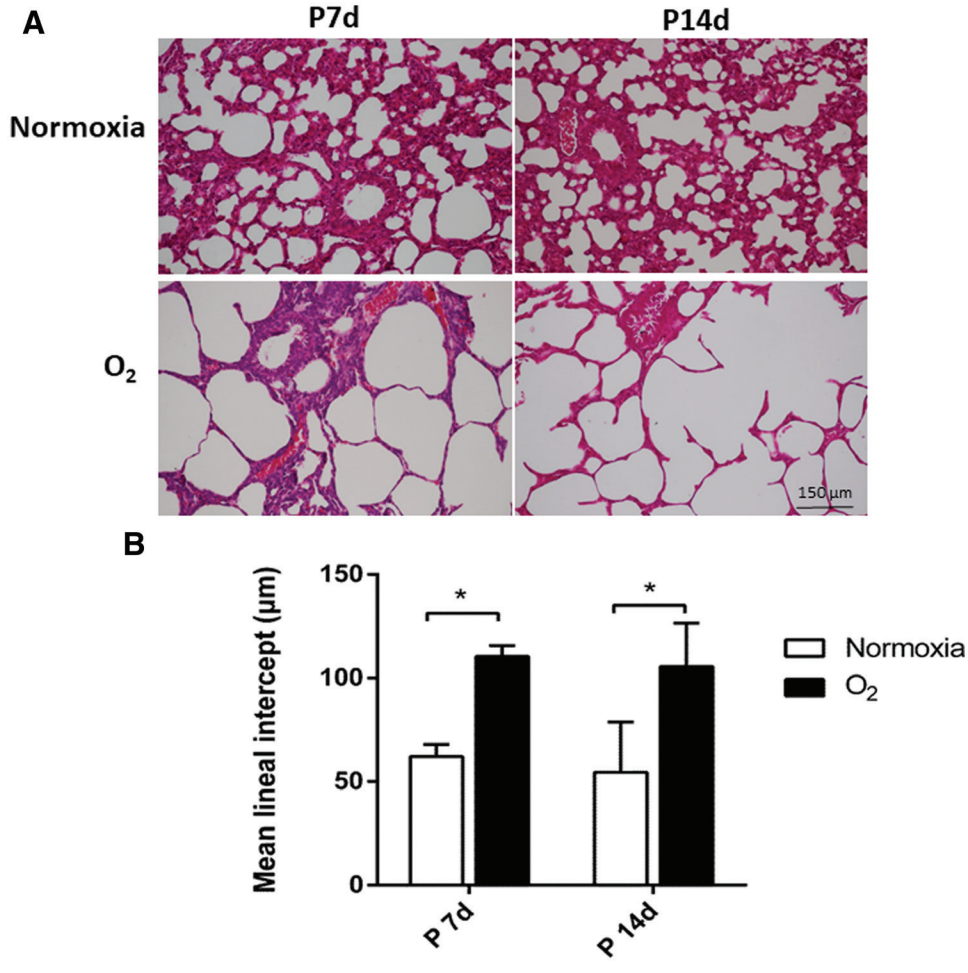

Fig. 1 Representative hematoxylin and eosin-stained lung sections for (A) histological observation and (B) mean linear intercept (MLI) assessment in the lungs of 7-day-old and 14-day-old rats in the normoxia and O_2-enriched groups. The rats in the O_2-enriched group exhibited a significantly higher MLI than those in the normoxia group. *$p < 0.05$.

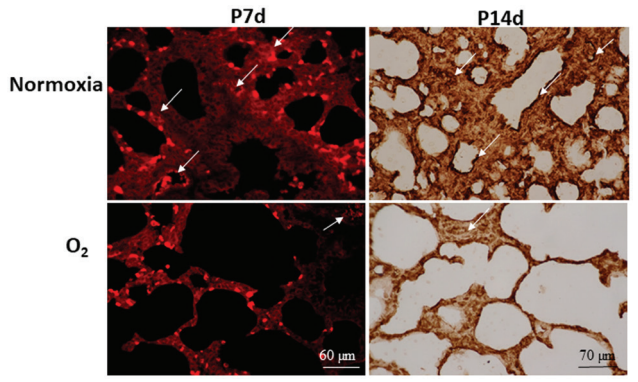

Fig. 2 (A) Representative lung sections of 7-day-old and 14-day-old rats in the normoxia and O_2-enriched groups stained with von Willebrand factor (vWF). White arrow indicates a positively stained vessel. The rats reared in hyperoxia showed reduced vWF-stained vessels than those reared in normoxia.

2.10. Statistical analysis

Data are presented as mean ± SD. Differences were analyzed using paired *t* test for *in vivo* data and one-way ANOVA for *in vitro* data, and analysis of significance was based on Bonferroni's correction for multiple comparisons. $p < 0.05$ indicated statistical significance.

3. RESULTS

3.1. Body weight, lung weight, and lung-to-body weight ratios

The rat pups in the O_2-enriched group exhibited significantly lower body and lung weights on postnatal days 7 and 14 than those in the normoxia group (Tables 1 and 2). Further, the rat pups in the O_2-enriched group exhibited a significantly lower lung-to-body weight ratio ($p < 0.01$) on postnatal day 7 and a significantly higher lung-to-body weight ratio ($p < 0.05$) on postnatal day 14 than those in the normoxia group.

3.2. Histological analyses

The lung sections of the normoxia group showed no major histological abnormalities, whereas those of the O_2-enriched group showed significantly higher MLI on postnatal days 7 and 14 ($p < 0.05$; Fig. 1).

3.3. Immunohistochemistry

Fig. 2 shows lung sections stained with vWF on postnatal days 7 and 14. The animals reared in the hyperoxic environment

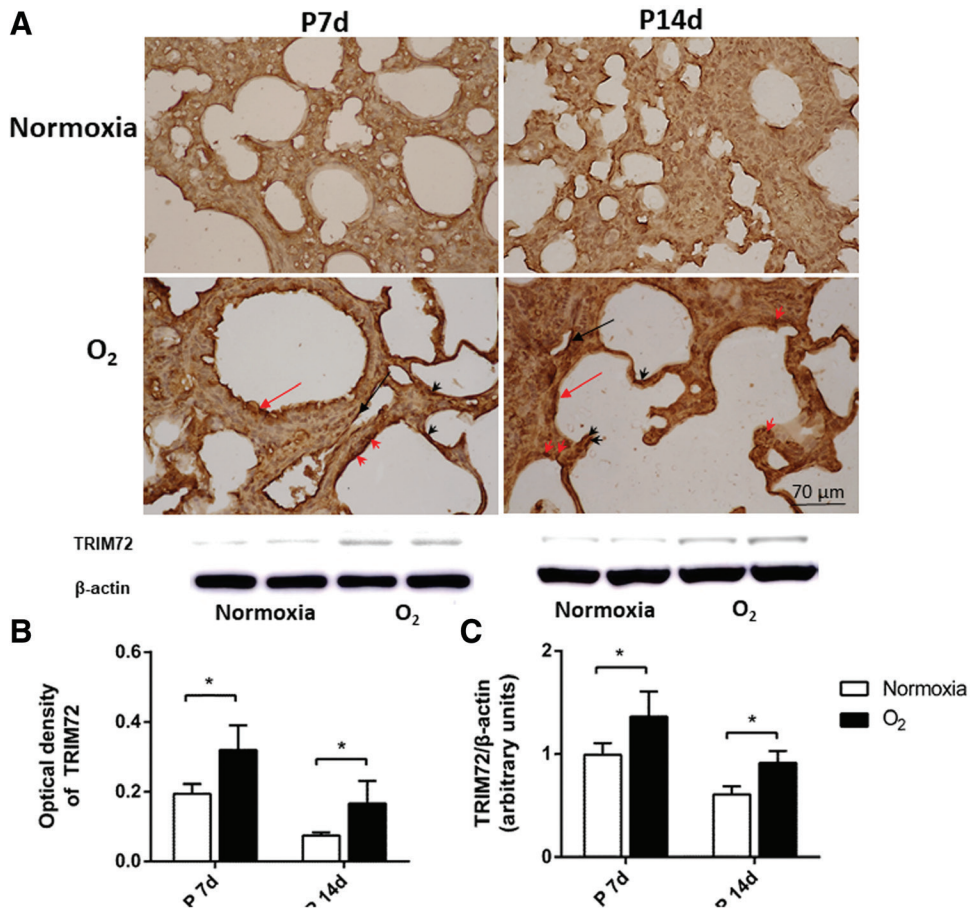

Fig. 3 Immunohistochemistry results (A) and Western blotting results and quantitative data (B, C) for TRIM72 expression in 7-day-old and 14-day-old rats in the normoxia and O_2-enriched groups. TRIM72 immunoreactivity was observed in endothelial cells (black arrow), superior surface of bronchial epithelial cells (red arrow), and alveolar type I (short black arrow) and II cells (short red arrow). The normoxia group showed faint immunoreactivity in bronchial epithelial cells (red arrow) and alveolar type I (short black arrow) and II cells (short red arrow). The rats in the O_2-enriched group exhibited significantly higher TRIM72 expression than those in the normoxia group on postnatal days 7 and 14. *$p < 0.05$.

showed decreased vWF-stained vessels than those reared in the normoxic environment.

TRIM72 immunoreactivity was observed in lung endothelial cells, superior surface of bronchial epithelial cells, and alveolar type I and II cells (Fig. 3A). The O_2-enriched group exhibited significantly higher TRIM72 immunoreactivity ($p<0.05$) than the normoxia group on postnatal days 7 and 14.

3.4. Western blotting

TRIM72 expression in rat lung tissues was analyzed using Western blotting. As shown in Fig. 3B and C, TRIM72 expression was significantly higher in the O_2-enriched group on postnatal days 7 and 14 ($p<0.05$).

3.5. O_2 exposure reduced the survival rate of lung cells

To investigate the effects of O_2 exposure on RLE-6TN and A549 cells, we performed the cell viability assay (MTT). The survival rate of both RLE-6TN and A549 cells significantly declined based on the duration of hyperoxia exposure ($p<0.001$). Interestingly, O_2-exposed TRIM72-siRNA RLE-6TN cells showed a sustained survival rate on days 2, 3, 4, and 5, whereas O_2-exposed TRIM72-siRNA A549 cells showed a sustained survival rate on days 3, 4, and 5 (Figs. 4A–D and 5A–D). By contrast, O_2-exposed TRIM72-adenovirus RLE-6TN and A549 cells showed a significantly lower survival rate on days 3, 4, and 5 and days 2, 3, 4, and 5, respectively (Figs. 4A–D and 5A–D). These results indicated that the effects of O2 on lung cells were attenuated or enhanced depending on whether TRIM72 expression was absent or present.

3.6. O_2 exposure enhanced TRIM72 expression

To investigate the effects of hyperoxia on TRIM72 expression in RLE-6TN and A549 cells, we cultured them under normoxia or O_2-enriched conditions for up to 120 hours. Thereafter, the cells were lysed and analyzed through ELISA. TRIM72 expression was significantly higher in O_2-exposed TRIM72-adenovirus RLE-6TN and A549 cells ($p<0.001$; Figs. 4E and 5E), whereas it was significantly attenuated in O_2-exposed TRIM72-siRNA RLE-6TN and A549 cells ($p<0.001$; Figs. 4E and 5E). Furthermore, TRIM72 expression was analyzed through Western blotting. The cells were cultured under normoxia or O_2-enriched conditions for up to 48 and 120 hours. TRIM72 expression was significantly increased in TRIM72-adenovirus A549 cells exposed to O_2 for 48 and 120 hours, whereas it was significantly attenuated in TRIM72-siRNA A549 cells exposed to O_2 for 48 and 120 hours ($p<0.05$ and $p<0.001$, respectively; Fig. 6A–C).

4. DISCUSSION

In this study, we found that rat pups exposed to hyperoxic conditions showed decreased body weight and lung weight

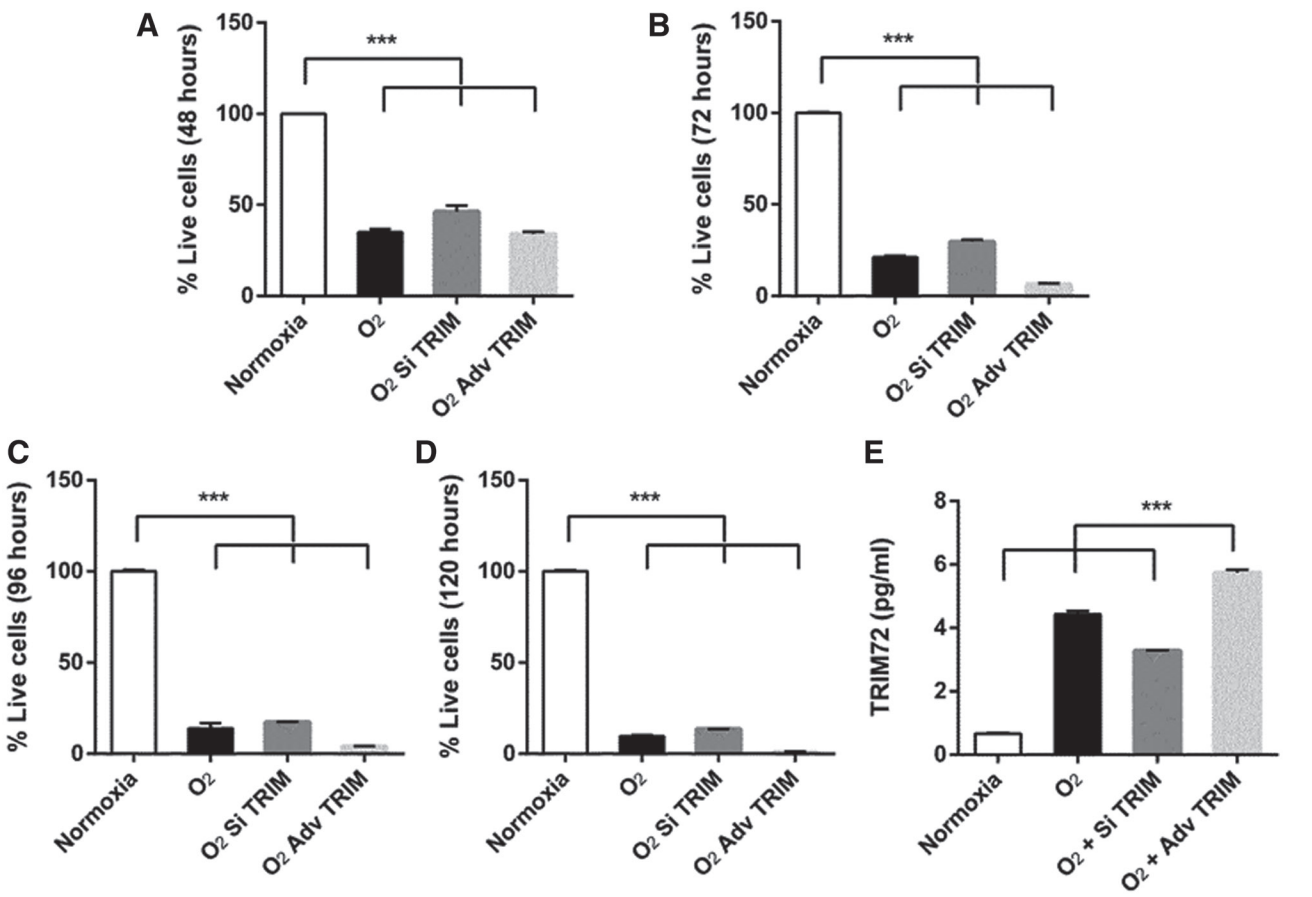

Fig. 4 O_2 exposure and lung cell viability and TRIM72 expression in RLE-6TN cells under normoxia, O_2, O_2+TRIM72 siRNA, and O_2+TRIM72 adenovirus were measured at (A) 48 h, (B) 72 h, (C) 96 h, and (D) 120 h. Cell viability was evaluated by measuring the mitochondrial-dependent reduction of colorless 3-(4, 5-dimethylthiazol-2-yl)-2, 5-diphenyltetrazolium bromide, normalized to cell number. At 120 h, we tested TRIM72 expression with ELISA. Bar graphs represent concentration (E). ***$p<0.001$.

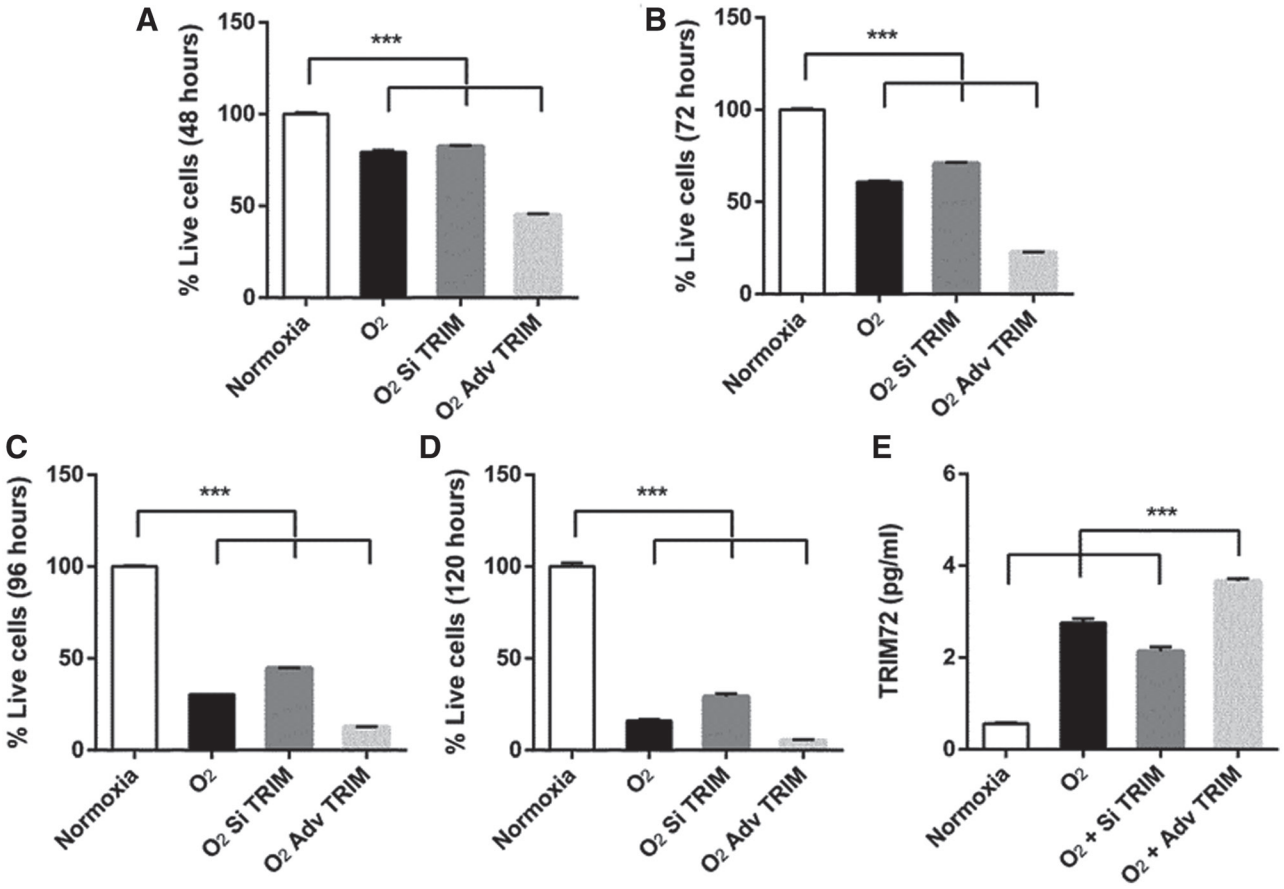

Fig. 5 O_2 exposure and lung cell viability and TRIM72 expression in A549 cells under normoxia, O_2, O_2+TRIM72 siRNA, and O_2+TRIM72 adenovirus were measured at (A) 48h, (B) 72h, (C) 96h, and (D) 120h. Cell viability was evaluated by measuring the mitochondrial-dependent reduction of colorless 3-(4, 5-dimethylthiazol-2-yl)-2, 5-diphenyltetrazolium bromide, normalized to cell number. At 120h, we tested TRIM72 expression with ELISA. Bar graphs represent concentration (E). ***$p<0.001$.

on postnatal days 7 and 14; furthermore, staining their lung tissues revealed increased MLI values and decreased vWF-stained vessels on postnatal days 7 and 14. Earlier studies have provided similar results.[19] TRIM72 expression in lung tissues under hyperoxic conditions was higher than that under normoxia on postnatal days 7 and 14. Furthermore, the attenuation or induction of TRIM72 expression in response to hyperoxia seemed to enhance or suppress the viability of cultured lung cells. Similar results have been provided by experimental studies that have investigated the outcome of different interventions on O_2-induced neonatal lung injury and animal models of BPD.[20,21]

BPD directly affects the lungs and is characterized by reduced alveolar and vascular growth and perturbed matrix remodeling. In the lungs, a considerable number of alveoli become fibrotic, scarred, and stop functioning. This affects not only the existing alveoli but also those that constantly develop after birth.[2] Previous studies have reported that hyperoxia exposure for 7 days increases oxidative stress in neonatal murine lungs.[22–24] Perturbed matrix remodeling and inflammation favoring fibrosis and an increase in septal thickness are typical features of hyperoxia-induced lung injury.[25] In an animal model of BPD, elastic fibers were noted in alveolar walls, contributing to the thickness of developing septa. Upon hyperoxia exposure, multiple signaling pathways determine the pulmonary cellular response: apoptosis, necrosis, fibrosis, or repair.[26] Further, experimental studies have demonstrated that the profibrotic signaling pathway involving transforming growth factor-β, phosphorylated signal transducer, and activator of transcription 3, and Smad2 is activated in response to hyperoxia.[5,25,27] The profibrotic signaling pathway plays a key role in increasing the thickness of alveolar septa. In this study, our results validated that exposure to hyperoxia causes impaired alveolar septa development and vascular formation that was indicated by an increase in alveolar MLI and a decrease in vWF-stained vessels.

TRIM72 expression can be induced by several experimental interventions, such as scratch wound, acute lung injury, and cardiac hypertrophy.[15,18,28] In this study, we found that TRIM72 expression was significantly upregulated in O_2-exposed TRIM72-adenovirus RLE-6TN and A549 cells, implying that TRIM72 was mainly expressed in bronchial epithelial cells and alveolar type I and II cells in our neonatal BPD model. TRIM72 expression was increased in the lung tissue of rat pups as well as rat alveolar cells and human lung epithelial cells subjected to hyperoxia. Accordingly, in a hyperoxic environment, TRIM72 may have an irreversible effect on lung cells, despite its cell membrane repair function.

TRIM72 overexpression contributes to cardiac fibrosis by regulating signal transducer and activator of transcription 3/Notch-1 signaling. Multiple signaling pathways also been implicated in cardiac fibrosis, including pathways involving transforming growth factor-β, the renin–angiotensin–aldosterone system, endothelin-1, and inflammatory and interferon receptors.[29] In this study, TRIM72 overexpression induced by

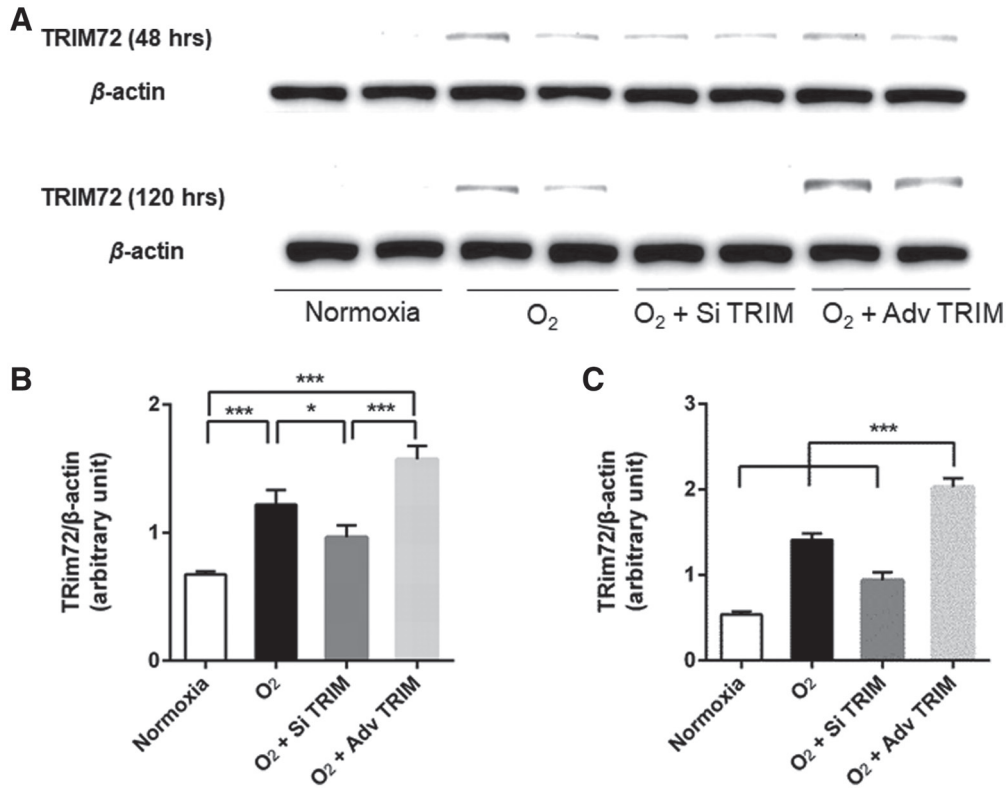

Fig. 6 Western blotting results (A) and quantitative data (B, C) of TRIM72 expression in A549 cells under normoxia, O_2, O_2+TRIM72 siRNA, and O_2+TRIM72 adenovirus were measured at 48 h (B) and 120 h (C). $^*p<0.05$, $^{***}p<0.001$.

TRIM72–GFP adenovirus decreased the viability of human and murine lung cells, and TRIM72 knockdown by TRIM72 siRNA increased their viability (Figs. 4A–D and 5A–D). We believe that the impairment of alveolar septa development and lung cell survival during hyperoxia contributed to the effects of TRIM72 on fibroblast proliferation and extracellular matrix remodeling through the profibrotic signaling pathway. Thus, the suppression of TRIM72 expression seems to be an effective approach to prevent hyperoxia-induced lung injury.

This study had two limitations: first, we determined cell culture viability to demonstrate the effects of O_2 exposure, and second, we used cell line cultures rather than primary cell cultures, which are less homogeneous relative to cell lines and have a limited lifespan as a consequence of being outside of their tissue niche. Future studies should use TRIM72-knockout animals and recombinant TRIM72 to further investigate the role of TRIM72 in hyperoxia-induced lung injury.

In conclusion, we herein report an important role of TRIM72 in hyperoxia-exposed lung tissues. TRIM72 overexpression or suppression may affect cell viability under hyperoxic conditions. Enhanced expression of TRIM72 can lead to alveolar and lung tissue changes and even influence weight and lung growth. Our study results suggest that the targeted suppression of TRIM72 can be a valuable new method to treat neonatal hyperoxia-induced lung injuries.

ACKNOWLEDGMENTS

This study was supported by grants from the Ministry of Science and Technology in Taiwan (MOST106-2314-B-038-085) and Taipei Medical University Regulations for Research Project Subsidies for Newly Appointed Faculty Members (TMU105-AE1-B22).

REFERENCES

1. Ramanathan R, Bhatia JJ, Sekar K, Ernst FR. Mortality in preterm infants with respiratory distress syndrome treated with poractant alfa, calfactant or beractant: a retrospective study. *J Perinatol* 2013;**33**:119–25.
2. Gien J, Kinsella JP. Pathogenesis and treatment of bronchopulmonary dysplasia. *Curr Opin Pediatr* 2011;**23**:305–13.
3. Jacob SV, Coates AL, Lands LC, MacNeish CF, Riley SP, Hornby L, et al. Long-term pulmonary sequelae of severe bronchopulmonary dysplasia. *J Pediatr* 1998;**133**:193–200.
4. Mouradian GC Jr, Alvarez-Argote S, Gorzek R, Thuku G, Michkalkiewicz T, Wong-Riley MTT, et al. Acute and chronic changes in the control of breathing in a rat model of bronchopulmonary dysplasia. *Am J Physiol Lung Cell Mol Physiol* 2019;**316**:L506–18.
5. Alejandre-Alcázar MA, Kwapiszewska G, Reiss I, Amarie OV, Marsh LM, Sevilla-Pérez J, et al. Hyperoxia modulates TGF-beta/BMP signaling in a mouse model of bronchopulmonary dysplasia. *Am J Physiol Lung Cell Mol Physiol* 2007;**292**:L537–49.
6. Bhandari V. Hyperoxia-derived lung damage in preterm infants. *Semin Fetal Neonatal Med* 2010;**15**:223–9.
7. Bhandari V. Molecular mechanisms of hyperoxia-induced acute lung injury. *Front Biosci* 2008;**13**:6653–61.
8. Wagenaar GT, ter Horst SA, van Gastelen MA, Leijser LM, Mauad T, van der Velden PA, et al. Gene expression profile and histopathology of experimental bronchopulmonary dysplasia induced by prolonged oxidative stress. *Free Radic Biol Med* 2004;**36**:782–801.
9. Manji JS, O'Kelly CJ, Leung WI, Olson DM. Timing of hyperoxic exposure during alveolarization influences damage mediated by leukotrienes. *Am J Physiol Lung Cell Mol Physiol* 2001;**281**:L799–806.
10. Chen CM, Wang LF, Chou HC, Lang YD, Lai YP. Up-regulation of connective tissue growth factor in hyperoxia-induced lung fibrosis. *Pediatr Res* 2007;**62**:128–33.
11. Seay U, Sedding D, Krick S, Hecker M, Seeger W, Eickelberg O. Transforming growth factor-beta-dependent growth inhibition in primary vascular smooth muscle cells is p38-dependent. *J Pharmacol Exp Ther* 2005;**315**:1005–12.

12. Stenmark KR, Abman SH. Lung vascular development: implications for the pathogenesis of bronchopulmonary dysplasia. *Annu Rev Physiol* 2005;**67**:623–61.
13. Song R, Peng W, Zhang Y, Lv F, Wu HK, Guo J, et al. Central role of E3 ubiquitin ligase MG53 in insulin resistance and metabolic disorders. *Nature* 2013;**494**:375–9.
14. Kohr MJ, Evangelista AM, Ferlito M, Steenbergen C, Murphy E. S-nitrosylation of TRIM72 at cysteine 144 is critical for protection against oxidation-induced protein degradation and cell death. *J Mol Cell Cardiol* 2014;**69**:67–74.
15. Jia Y, Chen K, Lin P, Lieber G, Nishi M, Yan R, et al. Treatment of acute lung injury by targeting MG53-mediated cell membrane repair. *Nat Commun* 2014;**5**:4387.
16. Zhao J, Lei H. Tripartite motif protein 72 regulates the proliferation and migration of rat cardiac fibroblasts via the transforming growth factor-β signaling pathway. *Cardiology* 2016;**134**:340–6.
17. Chen X, Su J, Feng J, Cheng L, Li Q, Qiu C, et al. TRIM72 contributes to cardiac fibrosis via regulating STAT3/Notch-1 signaling. *J Cell Physiol* 2019;**234**:17749–56.
18. Chou HC, Li YT, Chen CM. Human mesenchymal stem cells attenuate experimental bronchopulmonary dysplasia induced by perinatal inflammation and hyperoxia. *Am J Transl Res* 2016;**8**:342–53.
19. Chen CM, Hwang J, Chou HC. Maternal Tn immunization attenuates hyperoxia-induced lung injury in neonatal rats through suppression of oxidative stress and inflammation. *Front Immunol* 2019;**10**:681.
20. Alphonse RS, Vadivel A, Coltan L, Eaton F, Barr AJ, Dyck JR, et al. Activation of Akt protects alveoli from neonatal oxygen-induced lung injury. *Am J Respir Cell Mol Biol* 2011;**44**:146–54.
21. Park HS, Park JW, Kim HJ, Choi CW, Lee HJ, Kim BI, et al. Sildenafil alleviates bronchopulmonary dysplasia in neonatal rats by activating the hypoxia-inducible factor signaling pathway. *Am J Respir Cell Mol Biol* 2013;**48**:105–13.
22. Ishino H, Kawahito Y, Hamaguchi M, Takeuchi N, Tokunaga D, Hojo T, et al. Expression of Tn and sialyl Tn antigens in synovial tissues in rheumatoid arthritis. *Clin Exp Rheumatol* 2010;**28**:246–9.
23. Bouch S, O'Reilly M, Harding R, Sozo F. Neonatal exposure to mild hyperoxia causes persistent increases in oxidative stress and immune cells in the lungs of mice without altering lung structure. *Am J Physiol Lung Cell Mol Physiol* 2015;**309**:L488–96.
24. Valencia AM, Abrantes MA, Hasan J, Aranda JV, Beharry KD. Reactive oxygen species, biomarkers of microvascular maturation and alveolarization, and antioxidants in oxidative lung injury. *React Oxyg Species (Apex)* 2018;**6**:373–88.
25. Will JP, Hirani D, Thielen F, Klein F, Vohlen C, Dinger K, et al. Strain-dependent effects on lung structure, matrix remodeling, and Stat3/Smad2 signaling in C57BL/6N and C57BL/6J mice after neonatal hyperoxia. *Am J Physiol Regul Integr Comp Physiol* 2019;**317**:R169–81.
26. Mach WJ, Thimmesch AR, Pierce JT, Pierce JD. Consequences of hyperoxia and the toxicity of oxygen in the lung. *Nurs Res Pract* 2011;**2011**:260482.
27. Dasgupta C, Sakurai R, Wang Y, Guo P, Ambalavanan N, Torday JS, et al. Hyperoxia-induced neonatal rat lung injury involves activation of TGF-{beta} and Wnt signaling and is protected by rosiglitazone. *Am J Physiol Lung Cell Mol Physiol* 2009;**296**:L1031–41.
28. Li H, Duann P, Lin PH, Zhao L, Fan Z, Tan T, et al. Modulation of wound healing and scar formation by MG53 protein-mediated cell membrane repair. *J Biol Chem* 2015;**290**:24592–603.
29. Travers JG, Kamal FA, Robbins J, Yutzey KE, Blaxall BC. Cardiac fibrosis: the fibroblast awakens. *Circ Res* 2016;**118**:1021–40.